Electronic Supplementary Material (ESI) for Physical Chemistry Chemical Physics.

Electronic Supporting information for

Kamlet-Taft solvent parameters, NMR spectroscopic analysis and thermoelectrochemistry of lithium-glyme solvate ionic liquids

Jeffrey J. Black, Andrew Dolan, Jason B. Harper and Leigh Aldous

Contents:

Compositions of solutions studied

Table S1. Comparison of different representations of the compositions of the systems analysed, excluding pure solvents.

System	Mole Ratio (Solv.(O):Li[Tf_2N])	Mole Ratio (Solv.:Li[Tf_2N])	Mole Fraction (Li[Tf_2N])	Molality / mol kg^{-1}
T 0.025	40:1	40:1	0.024	0.347
G1 0.025	40:1	20:1	0.048	0.555
G2 0.025	40:1	40:3	0.070	0.559
G3 0.025	40:1	10:1	0.091	0.561
G4 0.025	40:1	8:1	0.111	0.562
T 0.25	4:1	4:1	0.200	3.467
G1 0.25	4:1	2:1	0.333	5.548
G2 0.25	4:1	4:3	0.429	5.590
G3 0.25	4:1	1:1	0.500	5.611
G4 0.25	4:1	4:5	0.556	5.624

T = THF; G1-4 = mono- to tetra-glyme

Calculation of Kamlet-Taft solvent parameters

Kamlet-Taft parameters were calculated using three solochromate dyes and the general formula below.

$$\nu_{\max} = \nu_{\max,0} + a\,\alpha + b\,\beta + s\,\pi^*$$

First the π^* parameter was determined using *N*,*N*-diethyl-4-nitroanaline which has an "*a*" and "*b*" value of 0 resulting in a solvochromatic shift dependent solely upon the π^* value. This allows determination of the π^* parameter through the following formula:

$$\pi^* = \frac{27.52 - \frac{10000\ nm}{\lambda_{max}}}{3.182}$$

Next Reichardt's dye, with a "*b*" value of 0, and 4-nitroanaline with an "*a*" value of 0 were used to determine the α and β parameters respectively using the absorption maxima and the previously obtained π^* value, using the following formulae:

$$\alpha = \frac{\frac{10000\ nm}{\lambda_{max}} - 74.58 + 1.873(34.12 - 2.343\ \pi^*)}{6.24}$$

$$\beta = \frac{1.035\ (27.52 - 3.182\ \pi^*)\ + 2.64 - \frac{10000\ nm}{\lambda_{max}}}{2.8}$$

Formulae and constants are derived from the literature[1-3] and have been left in this format to show how they were obtained. λ_{max} refers to the absorbance maximum for the dye of interest (Reichardt's dye for α, 4-nitroaniline for β and *N*,*N*-diethyl-4-nitroaniline for π^*).

Representative example of UV-Vis measurements for calculation of Kamlet-Taft parameters.

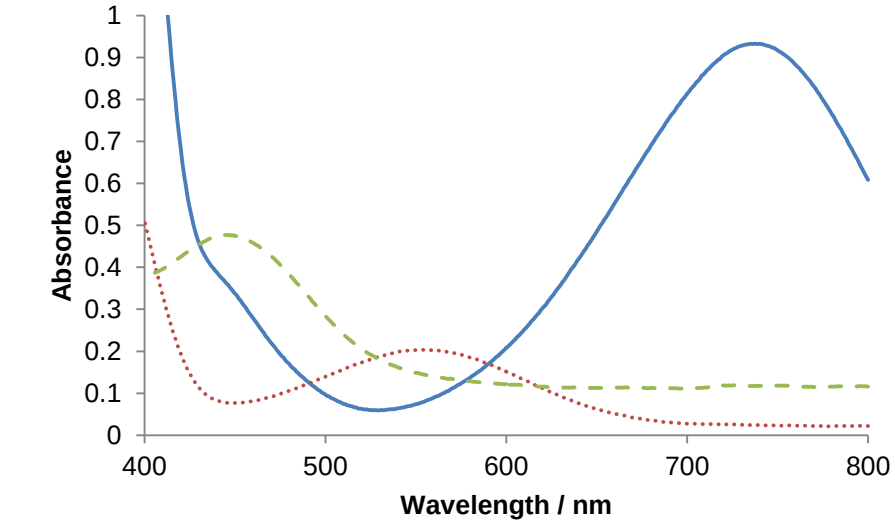

a

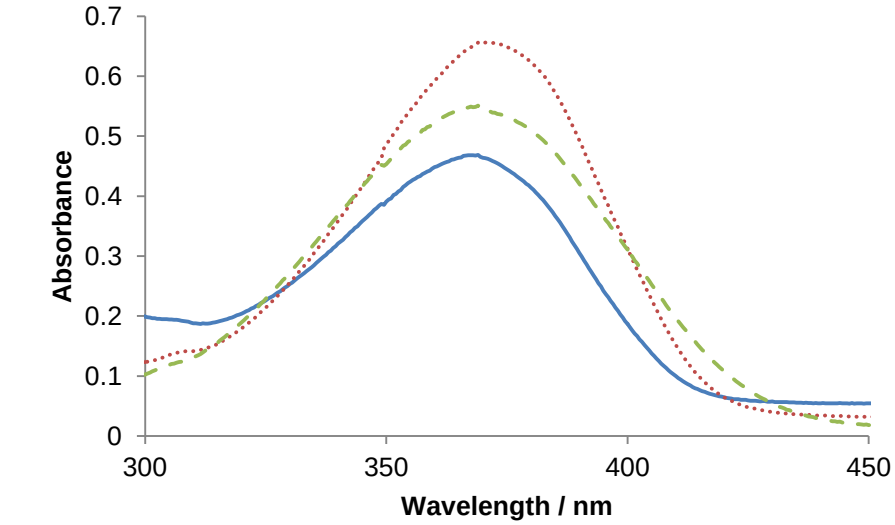

b

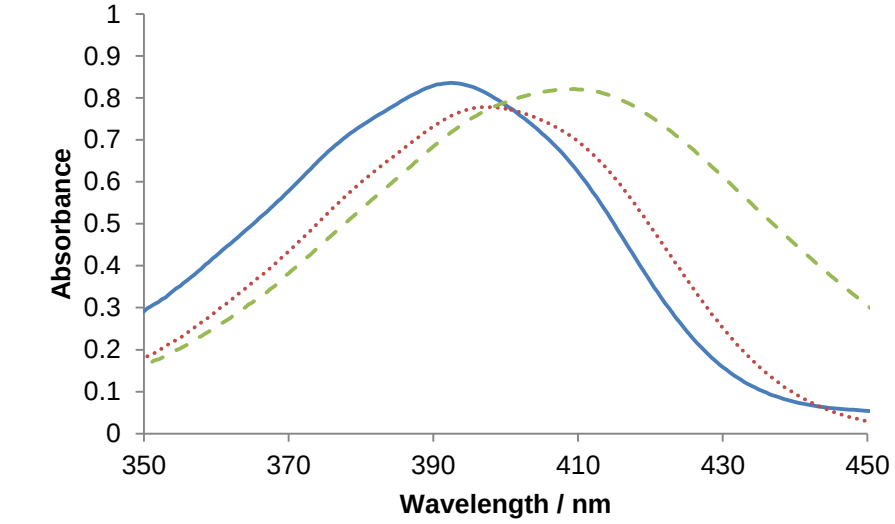

c

Figure S1. Solvachromatic shifts for G2 based systems, showing G2 (-), G2 0.025 (···) and G2 0.25 (- - -); for Reichardt's dye (a), 4-nitroaniline (b) and *N*,*N*-diethyl-4-nitroaniline (c).

Representative NMR spectra

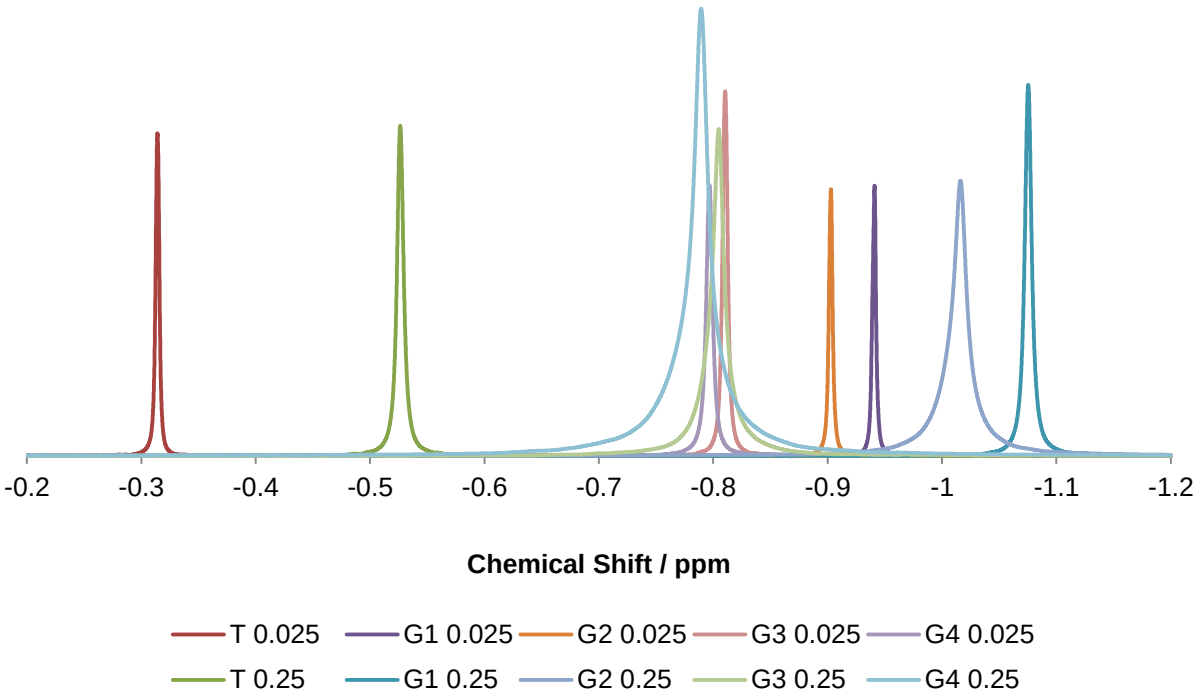

Figure S2. Lithium NMR spectra of Li[Tf_2N] solutions studied, showing significant changes in chemical shift for THF, G1 and G2, and similar chemical shifts for G3 and G4. Systems identified in graph legend indicating solvent used (T for THF, G1 through G4 for monoglyme to tetraglyme) and the number of solvent oxygens per lithium ion..

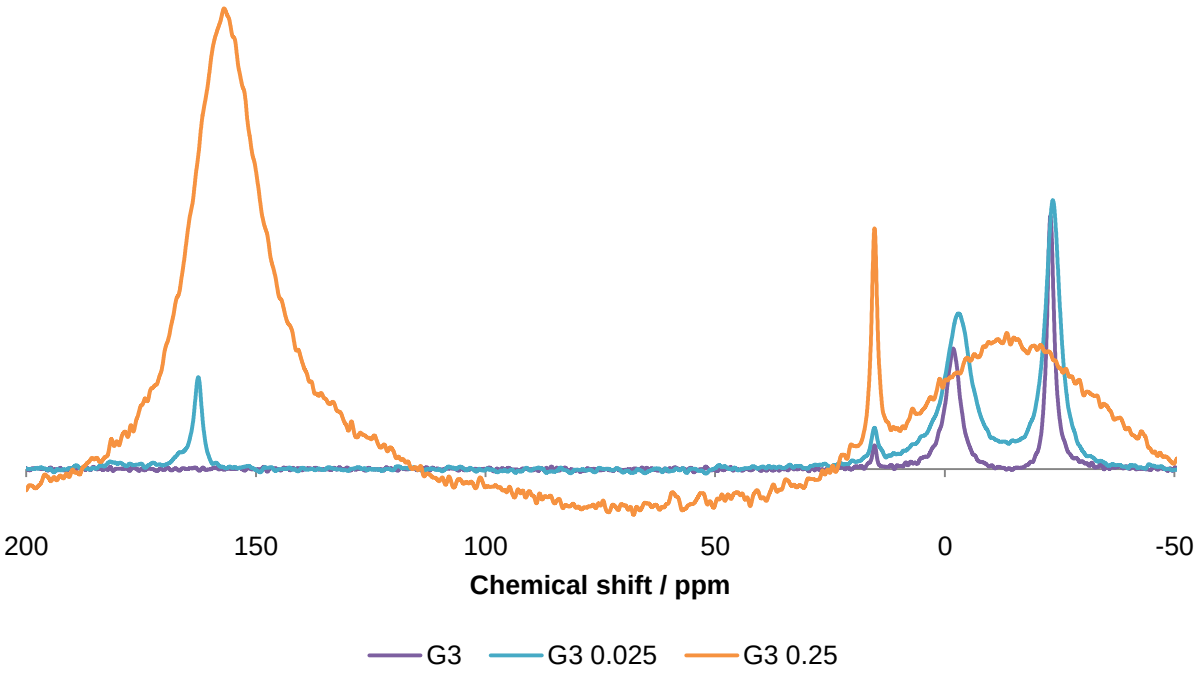

Figure S3. Representative ^{17}O NMR of the G3 systems (with the signal due to the Tf_2N^- anion on the left and the two signals due to the glyme on the right) showing very broad peaks for the concentrated salt case with only a single signal for the glyme. The remainining signal is the d_6-DMSO reference used.

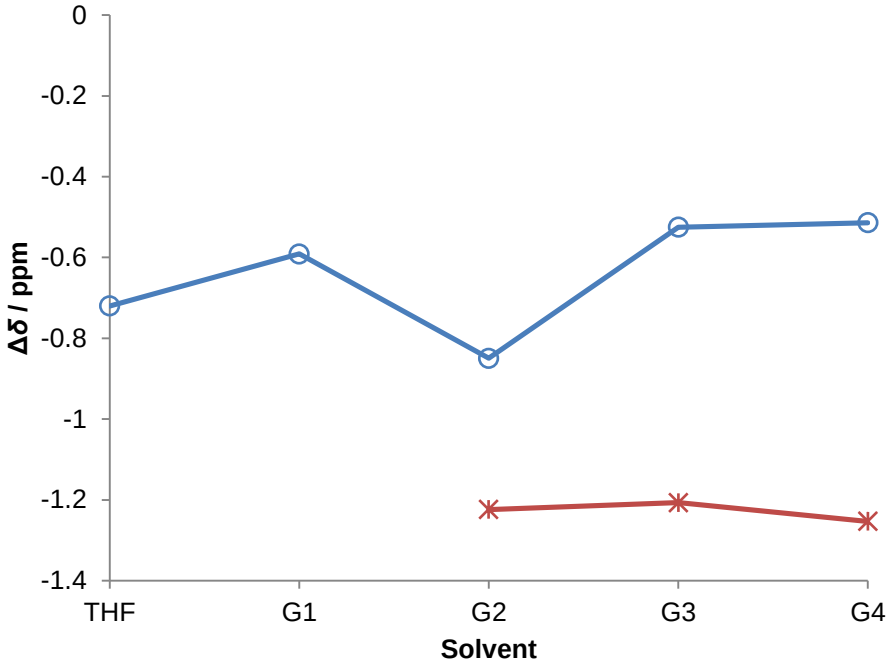

Figure S4. Change in ^{17}O NMR chemical shifts relative to pure solvents, of signals for terminal (blue circles) or non-terminal (red asterisk) oxygens in systems containing either THF, G1, G2, G3 or G4 with Li[Tf_2N] at a concentration corresponding to 0.025 lithium ions per solvent oxygen.

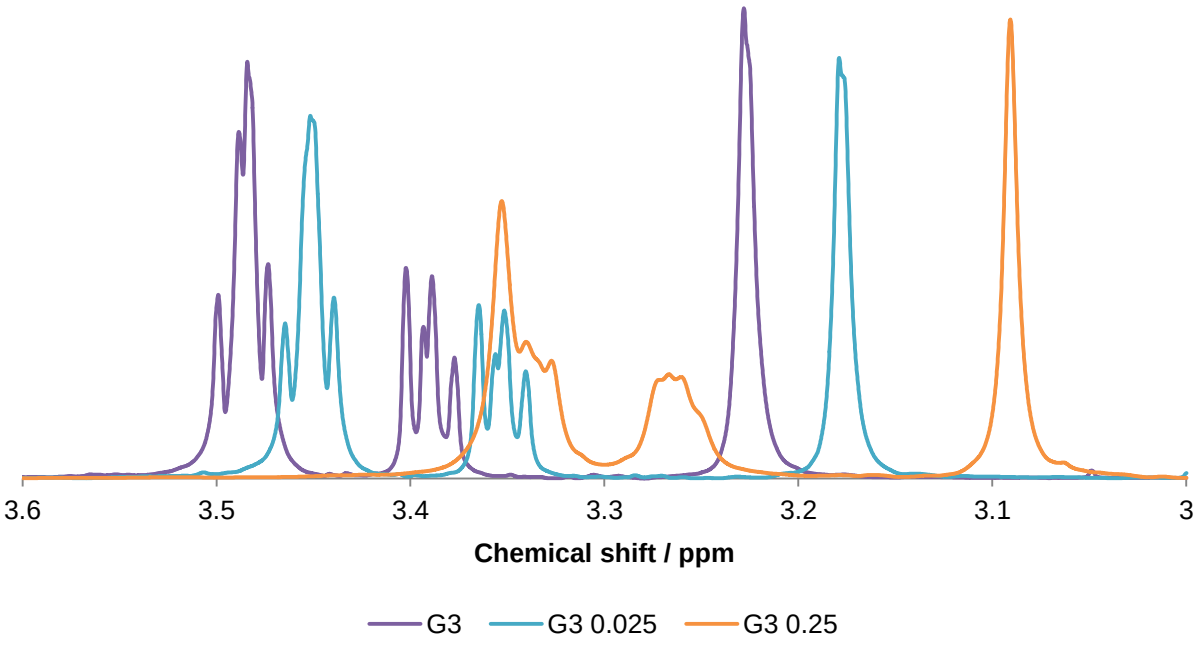

Figure S5. ^{1}H NMR signals for the glyme protons for the G3 systems, showing the significant change in chemical shift upon addition of Li[Tf_2N]. The signals due to the methyl protons are on the right and those due to the methylene protons are on the left; not all can be resolved as an individual signal in the latter case.

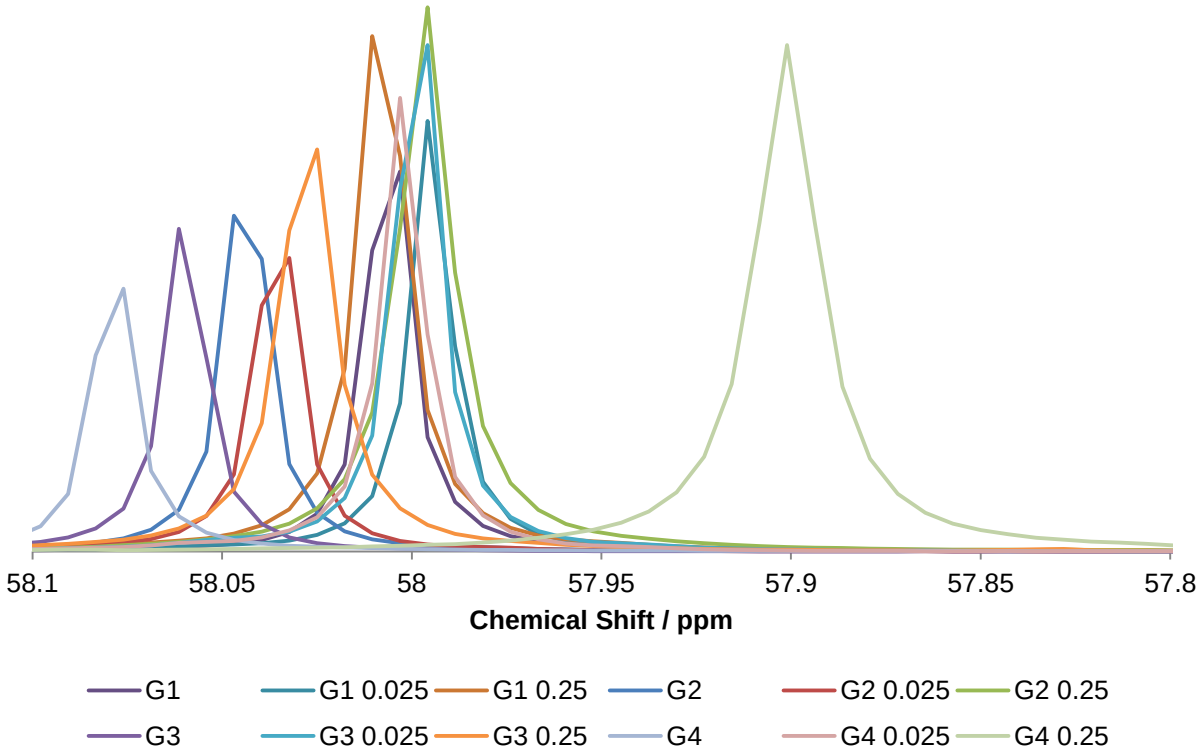

Figure S6. ^{13}C NMR signals correspondng to the gylme methyl groups in the pure glymes and Li[Tf_2N] solutions of the glymes, showing insignificant difference in chemical shifts between the glymes and upon addition of Li[Tf_2N].

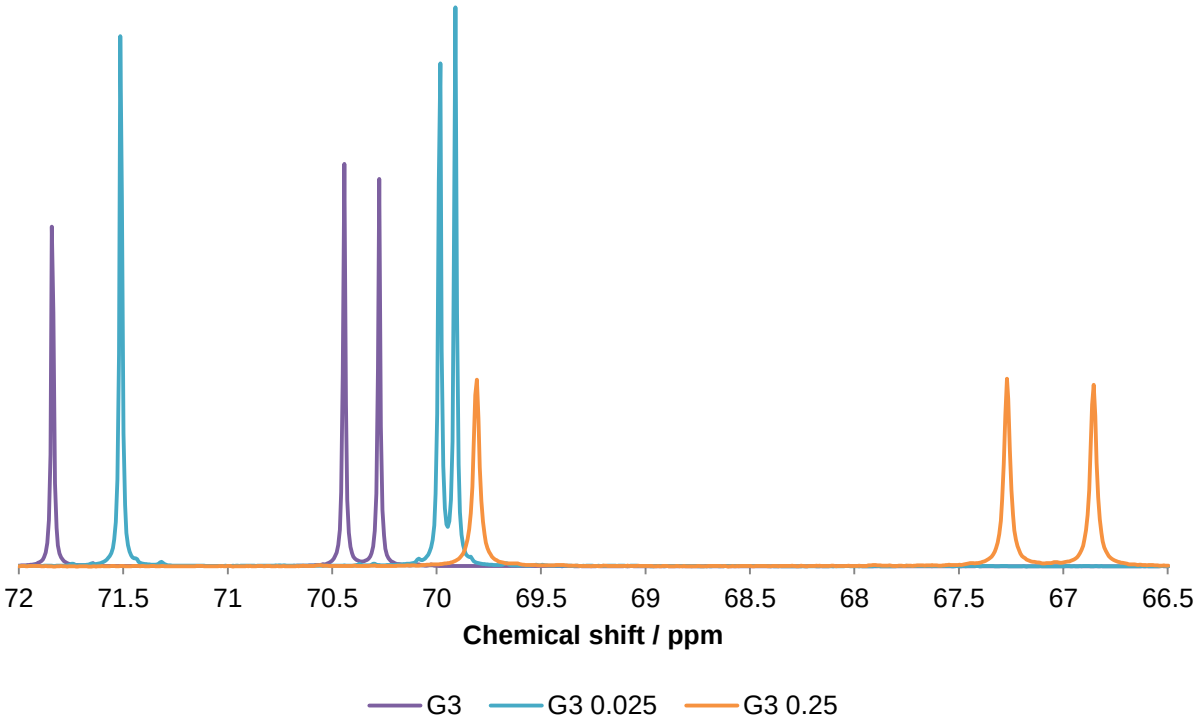

Figure S7. ^{13}C NMR signals correspondng to the methylene groups on G3, showing the significant chemical shift variations upon addition of Li[Tf_2N].

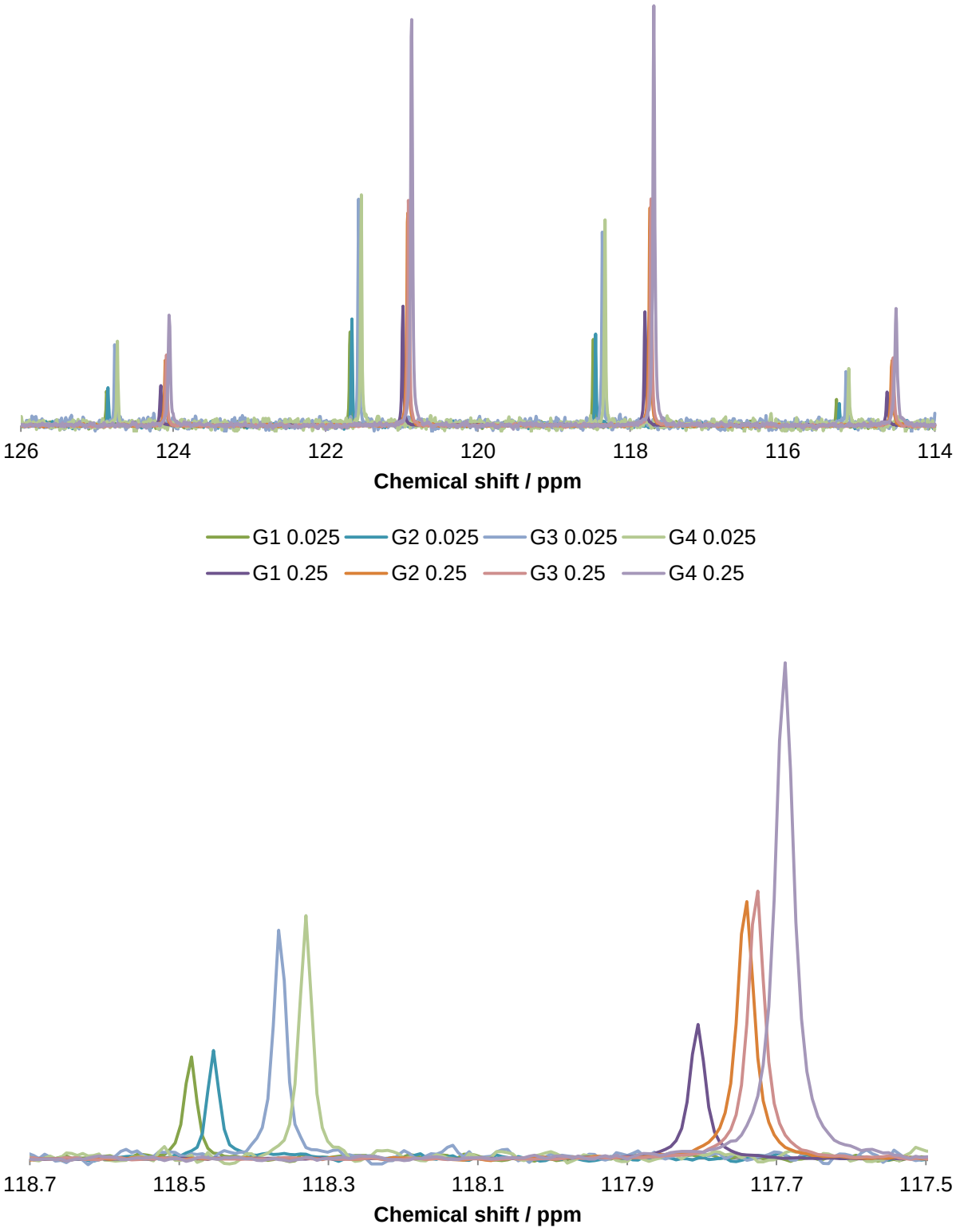

Figure S8. ^{13}C NMR signals due to Tf_2N^- anions in the Li[Tf_2N] solutions, including an enlagement of one of the signals, showing the negligble variation in signal position in the dilute and concentrated cases. Systems identified in figure legend as solvent (T for THF, G1 to G4 for monoglyme to tetraglyme) and number of solvent oxygen atoms per lithium ion.

Table of NMR chemical shifts

Table S2. NMR chemical shifts of systems studied. The ^{1}H 4+ column corresponds to the signal for the protons adjacent to the C 4, C 6 and C 7 carbons. Refer to Figure S9 for numbering.

System	^{7}Li	^{1}H 1	^{1}H 3	^{1}H 4+	^{13}C 1	^{13}C 3	^{13}C 4	^{13}C 6	^{13}C 7	^{17}O 2	^{17}O 5,8	^{13}C Tf_2N	^{17}O Tf_2N
THF		3.41	1.56		67.0					18.2			
T 0.025	-0.31	3.39	1.55		67.1					17.5		121.3	159.3
T 0.25	-0.53	3.36	1.47		67.5					12.0		121.0	157.4
G1		3.42	3.58		58.0	71.8				-23.2			
G1 0.025	-0.94	3.35	3.52		58.0	71.5				-23.8		121.7	160.5
G1 0.25	-1.08	3.14	3.32		58.0	69.9				-27*		121*	156*
G2		3.29	3.45	3.54	58.0	71.9	70.3			-22.9	-1.8		
G2 0.025	-0.90	3.24	3.40	3.50	58.0	71.6	70.0			-23.8	-3.0	121.7	162.8
G2 0.25	-1.02	3.08	3.26	3.35	58.0	69.5	68.1					121*	159*
G3		3.23	3.38	3.48	58.1	71.8	70.3	70.4		-23.0	-1.8		
G3 0.025	-0.81	3.18	3.35	3.45	58.0	71.5	69.9	70.0		-23.5	-3.0	121.6	162.5
G3 0.25	-0.80	3.09	3.26	3.33	58.0	69.8	66.9	67.3				121*	156*
G4		3.16	3.34	3.44	58.1	71.8	70.2	70.4	70.4	-23.1	-1.9		
G4 0.025	-0.80	3.14	3.31	3.41	58.0	71.5	69.9	70.0	70.0	-23.6	-3.1	121.5	162.7
G4 0.25	-0.79	3.05	3.23	3.35	57.9	69.5	67.3	67.6	67.8			121*	158*

*These ^{17}O signals were broad and thus are only quoted to 0 decimal places.

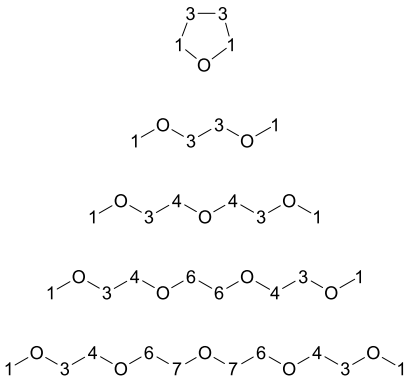

Figure S9. Numbering used for identification of atoms and corresponding signals for Table S2.

Seebeck Coefficient data

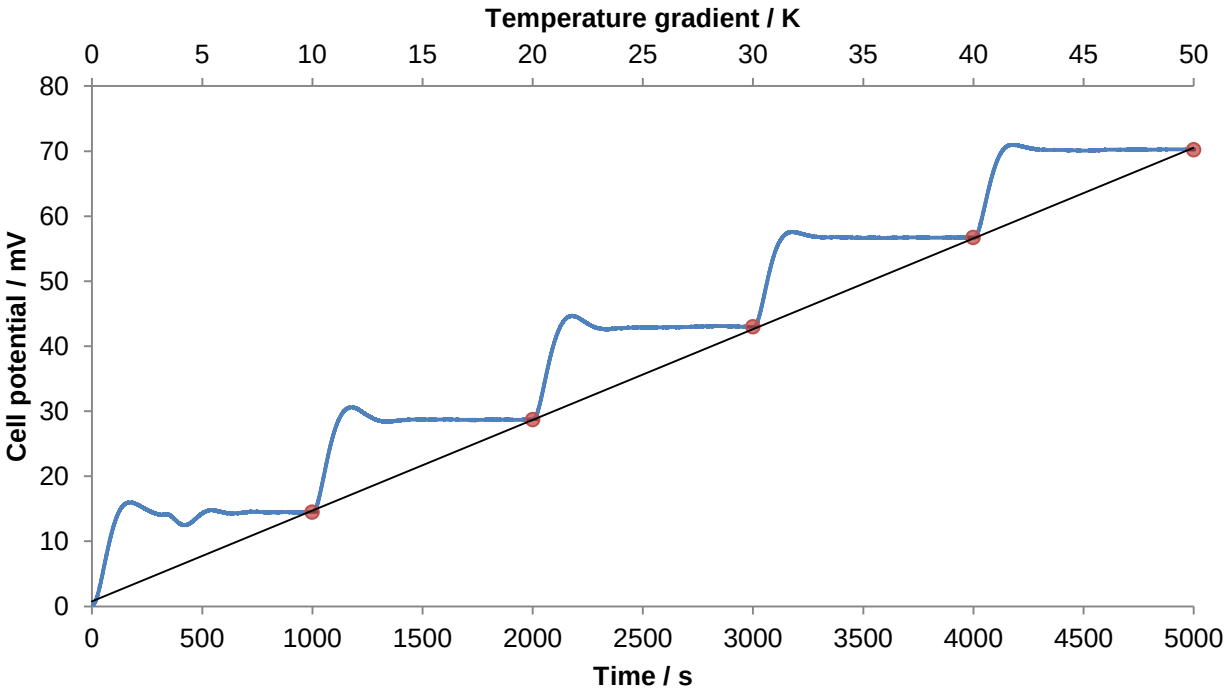

Figure S10. Raw open circuit potential measurement of a G3 0.025 cell, showing the resulting linear trend between temperature and cell potential.

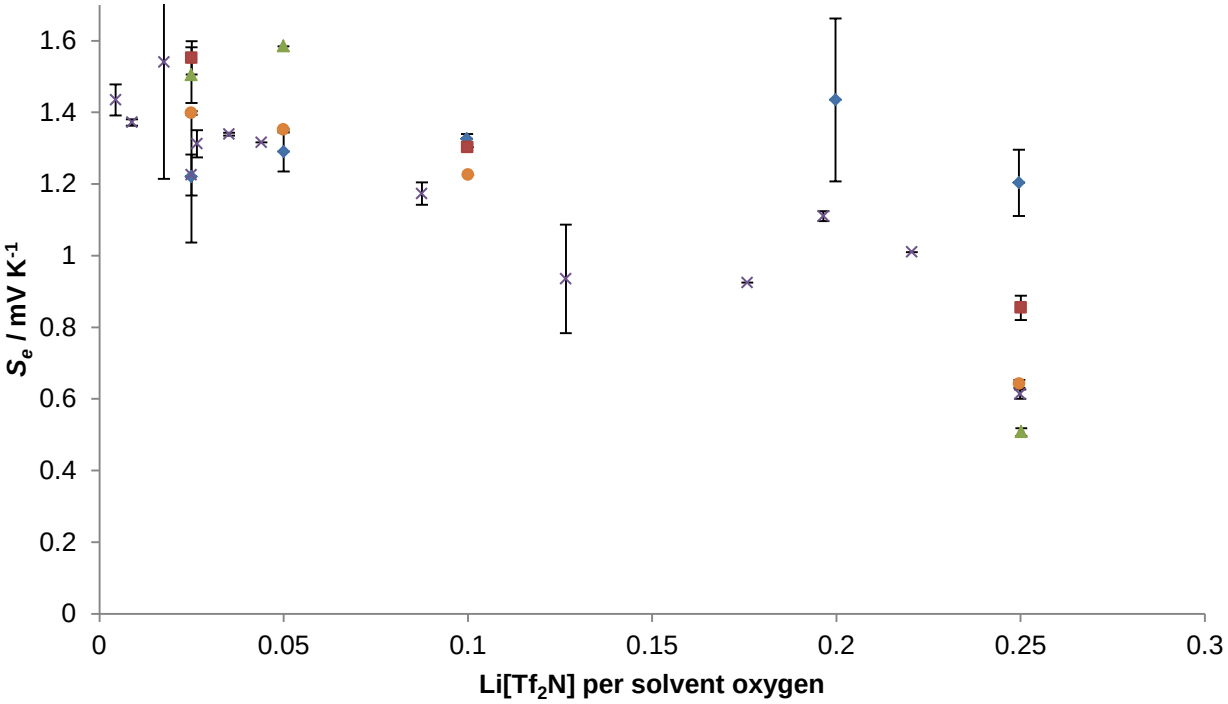

Figure S11. Seebeck coefficients of lithium metal electrodes in THF(◆), G1(■), G2(▲), G3(●) and G4(X) as a function of Li[Tf_2N] concentration.

Prediction of the solvation environment from the Seebeck coefficient

As discussed in the manuscript, the Seebeck coefficient is directly correlated with the entropy change occurring during the thermally-driven redox process. Solvent specific contributions to this entropy change relate to (i) immobilisation of solvent within the primary solvation sphere of the lithium cation, and (ii) partial immobilisation of the solvent within the secondary (Born) layer around the cation.

The Born entropy contribution was calculated using the equation:[4]

$$\Delta S_{\mathrm{Born}} = \frac{N_{\mathrm{A}}\, z^2 e^2}{8\,\pi\, r\, \varepsilon_0\, \varepsilon_{\mathrm{r}}^2} \frac{\mathrm{d}\varepsilon_{\mathrm{r}}}{\mathrm{d}T}$$

where N_A is Avogadro's constant z is the ion charge on the Li^+ (+1), e is the elementary charge, r is the hard sphere radius for Li^+ and a single layer of the solvent, ε_0 is the permittivity of free space, ε_r is the relative permittivity of the solvent, and $d\varepsilon_r/dT$ is the temperature dependence of the relative permittivity. The values in Table S3 were used. It should be noted that these are based upon approximations from available values. For example, the hard sphere radius is estimated assuming the Hard Sphere Volume of the equivalent alkanes, then extrapolating the radius assuming a spherical solvated ion (and including the Pauling ionic radii of the lithium cation). The relative permittivity is only applicable at infinite dilute, yet it is being employed here for relatively to extremely concentrated media. These calculations also neglects the role of the anion, especially given that contact ion pairs are expected. However, these are the only values available to estimate the solvation, and were employed impartially rather than matched to experimental observations.

Table S3. Calculation of Born entropic contribution to solvation.

Solvent	Hard sphere radius, r / nm	Relative permittivity, ε_r	Temperature dependence of the relative permittivity, $d\varepsilon_r/dT$	Calculated ΔS_{Born} / J K^{-1} mol^{-1}
THF	0.54	7.6	-0.029	-65
G1	0.70[£]	7.2	-0.029[&]	-55
G2	0.79[£]	7.3	-0.029[&]	-48
G3	0.86[£]	7.5	-0.029[&]	-42
G4	0.92[£]	7.7[$]	-0.029[&]	-37

[£] The Hard Sphere Radius was estimated from the van der Waal volumes of the equivalent alkanes,[5, 6]

[$] Estimated based upon extrapolating the values for G1, G2 and G3

[&] Literature value for THF assumed to apply to G1-G4.

Knowing the overall ΔS value from the Seebeck coefficent, and removing the ΔS value corresponding to either the loss or the formation of the ordered lithium metal phase and the estimated ΔS_{Born} contribution in solvent, the remaining ΔS value corresponds predominately to the ordering of the solvent in the primary solvation sphere. The solvent molecules are essentially 'frozen' in place when coordinating to the lithium cation, hence the entropy of fusion for a given solvent can be used to predict how many molecules (or what fraction of a molecule) was immoblised by the lithium cation, based upon the two ΔS values.

As such, the ΔS_{fus} value was predicted for each solvent at 293 K (the temperature of the cold electrode) using standard literature values (summarised in the Table below) and the below equation;

$$\Delta S^{\circ} = \Delta S_{\mathrm{fus}} + \Delta C_p \ln\left(\frac{293\ \mathrm{K}}{T_{\mathrm{fus}}}\right)$$

Table S4. Calculation of the entropy of fusion for the solvents used at 293 K.

Solvent	Temperature of Fusion, T_{fus} / K	Enthalpy of fusion, $\Delta H°$ / kJ mol^{-1}	Entropy of fusion, $\Delta S°$ / J K^{-1} mol^{-1}	Change in heat capacity upon phase transformation, ΔC_p / J K^{-1} mol^{-1}	Calculated entropy of fusion at 293 K, ΔS_{fus} / J K^{-1} mol^{-1}
THF	164.76[7]	8.54[7]	51.8[7]	-25.8[7]	37
G1	204[8]	8.49[8]	41.6*	33.4[@]	54
G2	209.1[8]	17.8[8]	85.1[9]	43.4[@]	100
G3	229.3[8]	23.71[8]	103.4[9]	53.4[@]	116
G4	243.45[8]	25.397[8]	104.3*	63.4[@]	116

* Calculated from the literature temperature of fusion and enthalpy of fusion values.

[@] Estimated change in the heat capacity upon fusion, based upon group contribution theory prediction of the heat capacity of the liquids and solids.[10]

There is known to be some thermal nonideality in the CR2032 battery casing, which has been discussed in depth elsewhere.[11] In order to correct for this, it was necessary to increase the overall entropy from the Seebeck coefficient by 27%. Subtracting the estimated phase change and Born entropy values from the overall ΔS value leaves a value which corresponds to immobilisation of the solvent in the inner sphere. Comparing this with the ΔS values for fusion of these solvents, an approximate number of solvent molecules immobilised in this inner solvation sphere can be calculated. This has been incuded in the table below, and is also expressed as equivalent solvent oxygens per lithium cation.

Table S5. Calculation of solvent oxygens immobilised by lithium ion.

System	Overall entropy from the Seebeck, ΔS / J K^{-1} mol^{-1}	Entropy corresponding to the inner solvation sphere, ΔS_{inner} / J K^{-1} mol^{-1}	Molecules in inner solvation sphere, based upon ΔS_{inner} / ΔS_{fus}	Equivalent solvent oxygen immobilised by lithium
T 0.025	150	127	3.4	3.4
G1 0.025	191	177	3.3	6.6
G2 0.025	185	179	1.8	5.4
G3 0.025	172	172	1.5	5.9
G4 0.025	152	157	0.5	6.8
T 0.25	148	125	3.4	3.4
G1 0.25	105	91	1.7	3.4
G2 0.25	62	56	0.6	1.7
G3 0.25	78	78	0.7	2.7
G4 0.25	76	81	0.2	3.5

Correlating Kamlet-Taft parameters to Seebeck coefficient

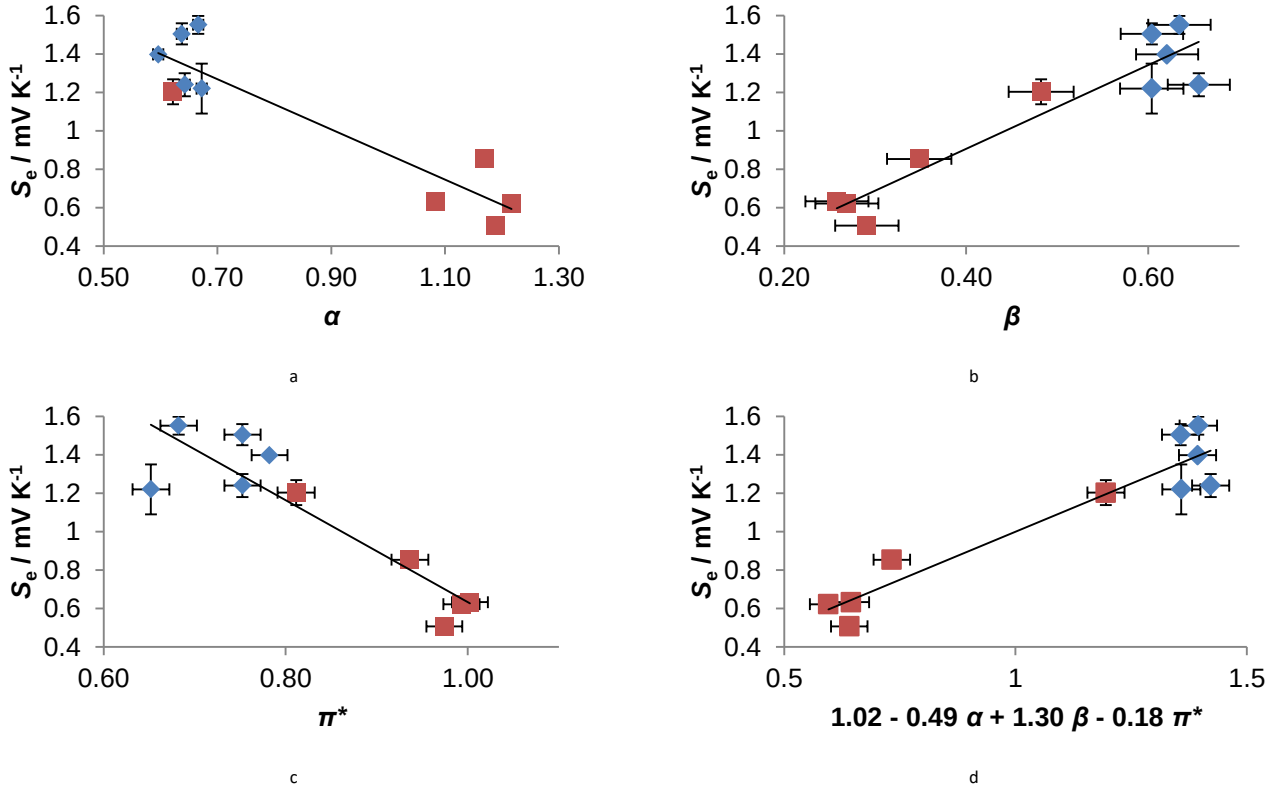

Figure S12. Correlations between Kamlet-Taft parameters and Seebeck coeffecient, showing the relation between the Seebeck coefficients and each of the Kamlet-Taft α (a), β (b), π^* (c) parameters individually, along with a linear combination of the three (d). Blue diamonds are the dilute solutions, red squares are the concentrated solutions.

Table S6. Linear Regression analysis results

Fitting equation	S_{e0} / mV K^{-1}	a / mV K^{-1}	b / mV K^{-1}	s / mV K^{-1}	R^2
$S_e=S_{e,0}+a\,\alpha$	2.18 ± 0.17	-1.31 ± 0.19			0.852305
$S_e=S_{e,0}+b\,\beta$	0.03 ± 0.14		2.18 ± 0.28		0.886317
$S_e=S_{e,0}+s\,\pi^*$	3.29 ± 0.38			-2.66 ± 0.45	0.816167
$S_e=S_{e,0}+a\,\alpha+b\,\beta+s\,\pi^*$	1.0 ± 1.6	-0.49 ± 0.50	1.3 ± 1.2	-0.2 ± 1.2	0.902413

References

1. R. W. Taft and M. J. Kamlet, *J. Am. Chem. Soc.*, 1976, **98**, 2886-2894.
2. M. J. Kamlet and R. W. Taft, *J. Am. Chem. Soc.*, 1976, **98**, 377-383.
3. M. J. Kamlet, J. L. Abboud and R. W. Taft, *J. Am. Chem. Soc.*, 1977, **99**, 6027-6038.
4. Y. Marcus, *J. Solution Chem.*, 1986, **15**, 291-306.
5. V. Gogonea, C. Bãleanu-Gogonea and E. Osawa, *J. Mol. Struct.: THEOCHEM*, 1998, **432**, 177-189.
6. Y. H. Zhao, M. H. Abraham and A. M. Zissimos, *J. Org. Chem.*, 2003, **68**, 7368-7373.
7. B. V. Lebedev, I. B. Rabinovich, V. I. Milov and V. Y. Lityagov, *J. Chem. Thermodyn.*, 1978, **10**, 321-329.
8. Z.-Y. Zhang, M. Frenkel, K. N. Marsh and R. C. Wilhoit, *Thermodynamic Properties of Organic Compounds and Mixtures · Enthalpies of Fusion and Transition of Organic Compounds*, Springer-Verlag, Berlin.
9. R. H. Beaumont, B. Clegg, G. Gee, J. B. M. Herbert, D. J. Marks, R. C. Roberts and D. Sims, *Polymer*, 1966, **7**, 401-417.
10. J. E. Hurst and B. Keith Harrison, *Chem. Eng. Commun.*, 1992, **112**, 21-30.
11. J. Wu, J. J. Black and L. Aldous, *Electrochim. Acta*, 2017, **225**, 482-492.